Thioredoxin Catalyzes the Denitrosation of Low-Molecular Mass and Protein *S*-Nitrosothiols†

Rajib Sengupta,‡ Stefan W. Ryter,§ Brian S. Zuckerbraun,‡ Edith Tzeng,‡ Timothy R. Billiar,‡ and Detcho A. Stoyanovsky*,‡

Departments of Surgery and Medicine, Division of Pulmonary, Allergy, and Critical Care Medicine, The University of Pittsburgh School of Medicine, Pittsburgh, Pennsylvania 15213

Received March 6, 2007; Revised Manuscript Received May 21, 2007

ABSTRACT: While most proteins have critical thiols whose oxidation affects their activity, it has been suggested that *S*-nitrosation and denitrosation of cellular thiols are fundamental processes similar to protein phosphorylation and dephosphorylation, respectively. However, understanding the biosynthesis and catabolism of *S*-nitrosothiols has proven to be difficult, in part because of the low stability of this class of metabolites. Herein, we report that thioredoxin catalyzes the denitrosation of a series of *S*-nitrosoamino acids and *S*-nitrosoproteins derived from HepG2 cells. Notably, all *S*-nitrosoproteins with a molecular mass of 23−30 kDa were catabolized by thioredoxin. Experimental evidence is presented which shows that both glutathione and reduced human thioredoxin denitrosate *S*-nitrosothioredoxin, which has been suggested to act as an anti-apoptotic factor via *trans*-*S*-nitrosation of caspase 3. In HepG2 cells, we observed that *S*-nitrosocysteine ethyl ester impedes the activity of caspase 3. However, a subsequent incubation of the cells in nitrosothiol-free medium resulted in reconstitution of the enzymatic activity, most likely due to endogenous denitrosation of *S*-nitrosocaspase 3. The latter process was markedly inhibited in thioredoxin reductase-deficient HepG2 cells, suggesting that the thioredoxin/thioredoxin reductase system tends to maintain intracellular caspase 3 in a reduced, SH state. The data obtained are discussed within the general reaction mechanisms encompassing the cellular homeostasis of *S*-nitrosothiols.

A considerable body of literature indicates that both nitric oxide (NO)-generating pharmacophores and endogenous NO production modulate the activity of proteins via reactions of *S*-nitrosation (*1*−*4*). Molecules with isolated thiol functions could be nitrosated to relatively stable *S*-nitrosothiols, whereas the nitrosation of vicinal thiols leads to intramolecular disulfide ring closure (*5*−*8*). While many proteins have critical thiols whose oxidation affects their activity, it has been suggested that *S*-nitrosation and denitrosation of cellular thiols are fundamental processes similar to protein phosphorylation and dephosphorylation, respectively (*9*, *10*). However, understanding the biosynthesis and catabolism of *S*-nitrosothiols (RSNOs)[1] has proven to be difficult, in part because RSNOs are short-lived metabolites. Three enzyme systems have been found thus far to catabolize *S*-nitrosoglutathione (GSNO): *Escherichia coli* and human thioredoxin (Trxn and HTrxn, respectively) (*11*), protein disulfide isomerase (PDI) (*12*), and alcohol dehydrogenase class III (ADH) (*13*). ADH does not catalyze the denitrosation of *S*-nitrosocysteine (CysSNO), *S*-nitrosohomocysteine (HCysSNO), or *S*-nitrosoalbumin (*13*), while the activity of PDI toward these low-molecular mass (LMM) RSNOs and *S*-nitrosoproteins remains to be established. However, excessive *S*-nitrosation of PDI isozymes has been associated with accumulation of misfolded proteins and neurodegeneration (*14*). Recently, we reported that Trxn catalyzes the denitrosation of *S*-nitrosated caspase 3, metallothionein, and albumin (Scheme 1; *7*). These studies suggest that specialized enzyme systems regulate the cellular levels of LMM and protein RSNOs.

In contrast to ADH and PDI, which are expressed mainly in the liver and kidneys (*4*) and in the lumen of the endoplasmic reticulum (*15*), respectively, Trxn is a ubiquitous protein (*16*, *17*). Trxn activity has been linked to cell growth, transcription factor regulation, DNA synthesis, protein binding (*16*, *18*, *19*), detoxification of free radicals (*20*), and regeneration of antioxidants (*21*). On the other hand, genetic deletion of Trxn in mice yields lethal phenotypes (*22*, *23*). Trxn contains a -Cys-Gly-Pro-Cys- motif that is essential for its enzyme activity. Cysteines 32 and 35 in

† This work was funded by U.S. Public Health Service Grants ES09648 (D.A.S.) and R37-GM44100 (T.R.B.) from the National Institutes of Health.

* To whom correspondence should be addressed: MUH-NW 654, Department of Surgery, University of Pittsburgh, 3459 Fifth Ave., Pittsburgh, PA 15213. Telephone: (412) 647 6087. Fax: (412) 647 5959. E-mail: stoyanovskyd@msx.upmc.edu.

‡ Department of Surgery.

§ Department of Medicine.

[1] Abbreviations: ADH, alcohol dehydrogenase; SNCEE, *S*-nitroso-L-cysteine ethyl ester; CysSNO, *S*-nitroso-L-cysteine; MSF, 5-[(*S*)-(+)-2-(methoxymethyl)pyrrolidino]sulfonylisatin; ANF, auronafin; DTNB, 5,5′-dithiobis(2-nitrobenzoic acid); GSH, reduced glutathione; GSNO, *S*-nitrosoglutathione; HCysSNO, *S*-nitroso-L-homocysteine; HPLC-EC, high-performance liquid chromatography with electrochemical detection; HPLC-SE, high-performance liquid chromatography with size exclusion; Trxn, *E. coli* thioredoxin; HTrxn, human thioredoxin; LA, lipoic acid; DHLA, dihydrolipoic acid; LMM, low-molecular mass; NMB, 2-nitro-5-mercaptobenzoic acid; RSNO, *S*-nitrosothiol; SNAP, *S*-nitroso-*N*-acetylpenicillamine; TrxnR, *E. coli* thioredoxin reductase.

10.1021/bi700449x CCC: $37.00
Published on Web 06/20/2007

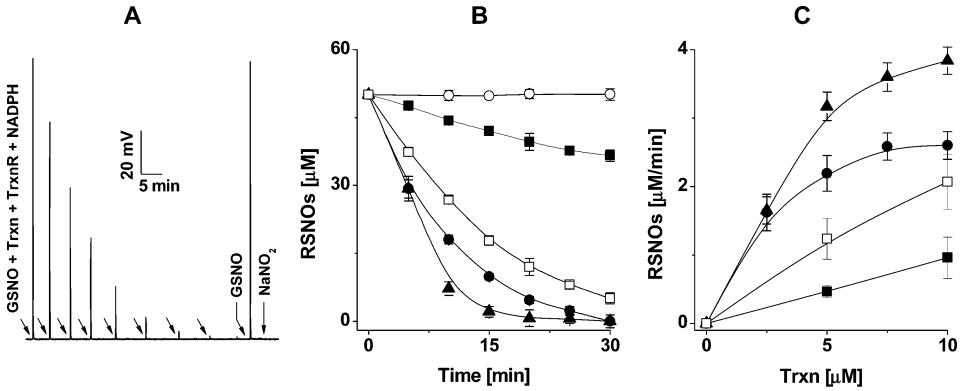

FIGURE 1: Trxn denitrosates LMM RSNOs. Reactions were carried out at 37 °C in 0.1 M phosphate buffer (pH 7.4) containing 0.1 mM EDTA. RSNOs, Trxn, TrxnR, NADPH, and $NaNO_2$ were used at concentrations of 50 μM, 5 μM, 0.08 μM (1 unit/mL), 0.4 mM, and 0.1 mM, respectively. RSNO quantification was performed as described in Experimental Procedures. The data in panels B and C are presented as mean values of three independent experiments ± the standard error. (A) Trxn-catalyzed denitrosation of GSNO. At given time points (arrows), aliquots from the reaction solution were assessed for GSNO content. (B) Trxn-catalyzed denitrosation of GSNO (●), CysSNO (▲), HCysSNO (□), SNAP (■), and GSNO, TrxnR, and NADPH (○). (C) Rates of RSNO denitrosation as a function of Trxn concentration: GSNO (●), CysSNO (▲), HCysSNO (□), and SNAP (■).

the active site of thioredoxin [$Trxn(SH)_2$] can reduce SS and SNO functions on substrate proteins with concomitant disulfide ring closure to $Trxn(S)_2$ and release of the reduced, SH form of the substrate protein. In turn, $Trxn(S)_2$ is converted back to $Trxn(SH)_2$ by the NADPH-dependent thioredoxin reductase [TrxnR (*7*, *16*)]. Proteomic analyses of wheat starchy endosperm and *E. coli* led to the identification of 80 proteins as potential targets of Trxn, which are involved in 26 distinct cellular processes (*24*, *25*). However, the specificity of Trxn toward protein disulfides and RSNOs in mammalian cells has not been studied well. Herein, we report that Trxn catalyzes the denitrosation of a series of LMM RSNOs and *S*-nitrosoproteins derived from HepG2 cells. Notably, Trxn exhibited particularly high catalytic activity in the in vitro denitrosation of *S*-nitrosoproteins with molecular masses of 23−30 kDa and catalyzed the denitrosation of *S*-nitrosocaspase 3 in HepG2 cells.

EXPERIMENTAL PROCEDURES

Reagents. All reagents were purchased from Sigma Chemical Co. (St. Louis, MO). Human RhoA protein was purchased from Cytoskeleton, Inc. (Denver, CO). The solutions used in the experiments were prepared in deionized and Chelex-100-treated water or potassium phosphate buffer.

Preparation of RSNOs. Nitrosation of CysSH, HCysSH, GSH, and L-cysteine ethyl ester to CysSNO, HCysSNO, GSNO, and *S*-nitroso-L-cysteine ethyl ester (SNCEE), respectively, was carried out with nitrosooxy ethane (C_2H_5ONO) as described previously (*26*). Briefly, the corresponding thiol (0.1−0.5 g) was dissolved in methanol (5 mL) containing C_2H_5ONO (0.5 mL; bp of 13 °C), and the reaction solutions were incubated for 30 min in ice. Thereafter, the solvent and the remaining C_2H_5ONO were rotor-evaporated at room temperature, and the nitrosothiol that formed was recrystallized from methanol. The purity of the nitrosothiols was assessed by UV spectrophotometry. At 550 nm, ϵ_{GSNO}, ϵ_{CysSNO}, and $\epsilon_{HCysSNO}$ = 16.1, 16.6, and 16.7 M^{-1} cm^{-1}, respectively (*27*); in methanol, $\epsilon_{(343)SNCEE}$ = 1019 M^{-1} cm^{-1} and $\epsilon_{(544)SNCEE}$ = 36 M^{-1} cm^{-1} (*26*).

Analysis of RSNOs. RSNOs were quantified following their Cu^+-catalyzed breakdown to RSH and NO with concomitant chemiluminescence measurements of the latter in the gas phase using a Sievers (Boulder, CO) nitric oxide analyzer (NOA 280i) (*28*). The purge vessel of the NO analyzer was filled with 5 mL of 0.1 M phosphate buffer (pH 7.4; 20 °C; carrier gas, He). In the reaction vessel, a steady-state concentration of Cu^+ was maintained by a large excess of ascorbic acid over $CuCl_2$ (50 mM vs 0.2 mM). Thus, multiple injections of aliquots (5−20 μL) containing RSNOs could be made without any significant loss of analytical sensitivity, as indicated by the release of NO after injection of a standard solution of GSNO upon completion of the reactions (Figure 1A). Under these experimental conditions, $NaNO_2$ (up to 0.1 mM) did not interfere with the analysis of RSNOs (Figure 1A). Calibration of the experimental peaks was performed by injection of standard solutions of either *S*-nitroso-*N*-acetylpenicillamine (SNAP) or GSNO (0.1−50 μM).

Determination of Levels of Proteins and Thiols. Protein concentrations in samples were determined using the Bio-Rad protein assay kit with bovine serum albumin as the standard. Protein thiols were assessed colorimetrically at 412 nm following the reduction of 5,5′-dithiobis-2-nitrobenzoic acid (DTNB) to 2-nitro-5-mercaptobenzoic acid (NMB) [ϵ_{412} = 13 500 M^{-1} cm^{-1} (*29*)]. In samples with a low content of thiols, NMB was quantified by HPLC with electrochemical (EC) detection. Isocratic separations were achieved with 15% methanol at a flow rate of 1 mL/min with C-18 reverse phase columns (Alltima, 4.6 mm × 250 mm, 5 μm; Alltech Associates, Inc., Deerfield, IL). EC detection was carried out with an LC-4C amperometric detector (Bioanalytical Systems, West Lafayette, IN) at a holding potential of 0.9 V. Under these chromatographic conditions, NMB exhibited a retention time (t_R) of 4.6 min.

Cell Culture and Treatments. Human hepatoma (HepG2) cells were cultured in Dulbecco's modified Eagle's medium supplemented with 10% fetal calf serum, 100 units/mL penicillin, 100 μg/mL streptomycin, and 2 mM L-glutamine in a humidified atmosphere of 5% CO_2 at 37 °C.

Caspase 3 Activation in HepG2 Cells. Cells (2×10^6 cells/flask) were grown in T75 flasks for 24 h and then incubated with paclitaxel (50 nM) for 24 h followed by a 24 h exposure to the Cdks inhibitor NU6140 [10 μM (*30*); Calbiochem,

San Diego, CA]. Alternatively, cells were incubated for 4.5 h with medium (control) or with medium containing 15 ng of TNF-α and 40 μM cycloheximide (CHX, from Sigma) (*31*). Thereafter, the cells were washed with PBS (3 × 10 mL) and incubated for 15 min at 37 °C with standard incubation medium containing SNCEE. Whole-cell lysates for analysis of caspase 3 were harvested by repeated freeze and thaw cycles followed by centrifugation at 15000*g* for 15 min at 4 °C.

Auranofin (AFN) Treatment. Approximately 2×10^5 cells were plated per well in a six-well plate. The following day, cells were incubated for 12 h at 37 °C in medium containing ANF (5 μM). Thereafter, the cells were washed with PBS (3 × 5 mL), and cell viability was determined using crystal violet staining.

Toxicity of SNCEE. For cytotoxicity experiments, HepG2 cells were plated at a density of 2×10^5 cells per well per 0.5 mL of tissue culture medium on 24-well tissue culture plates. After incubation and attachment for 12 h, SNCEE was added, and the cells were incubated for 6 h at 37 °C. Cell viability (cytotoxicity) was determined using crystal violet staining (*32*).

siRNA Transfection. The siRNA directed against TrxnR was 5′-AGACCACGUUACUUGGGCAdTdT-3′, and the control was a scrambled sequence (5′-AGGCAAAUCACG-GUGUCCUdTdT-3′) that does not match any sequence in the GenBank human database for >16 nucleotides (*33*; Dharmacon RNA Technologies, Chicago, IL). Approximately 2×10^5 HepG2 cells were plated per well in a six-well plate. The following day, siRNAs were transfected with lipofectamine 2000 (Invitrogen, Carlsbad, CA), with 30 pmol of siRNA per well (*34*), according to the manufacturer's recommendations. Transfection with the same amount of nonspecific siRNA was performed as a control. The cells were harvested and analyzed 24, 48, and 72 h after transfection for cell viability, activity, and level of TrxnR protein.

Protein S-Nitrosation. For isolation of proteins, HepG2 cells were disrupted by three cycles of freezing and thawing. The resulting homogenate was centrifuged for 90 min at 100000*g*, and LMM compounds were removed from the supernatant via ultrafiltration through a 10 kDa cutoff filter (Vivaspin 500, Cole Palmer, Vernon Hills, IL). The filtrate was discarded, while the protein fraction (~0.01 mL) was diluted with 0.1 M phosphate buffer (0.2 mL, pH 7.4) containing EDTA (0.2 mM) and subjected to a second ultrafiltration. The final protein extracts (5 mg of protein/mL; molecular mass of ≥10 kDa) were treated with GSNO (0.3 mM) for 30 min at 20 °C; then, the excess of GSNO was removed via ultrafiltration (10 kDa Vivaspin cutoff filter), which included four washing cycles with 0.1 M phosphate buffer containing 0.2 mM EDTA (4 × 0.2 mL). In the final protein fraction, the content of GSNO was less than 0.1 μM, as assessed by reverse phase HPLC-EC [C-18 column, Alltima 4.6 mm × 250 mm, 5 μm; Alltech Associates, Inc.; holding potential, 0.8 V; mobile phase, 50 mM phosphate buffer containing 10% CH_3OH; t_R(GSNO) = 3.9 min]. The *S*-nitrosoproteins thus obtained could be kept at −70 °C for up to 1 month without any significant losses of SNO functions.

S-Nitrosation of RhoA (18 μM), HTrxn-S_2 (0.4 mM), and caspase 3 was performed with GSNO (0.3−2 mM) at 20 °C for 30 min in 0.1 M phosphate buffer containing 0.2 mM EDTA. Thereafter, *S*-nitrosoproteins were separated from GSH and the excess of GSNO via ultrafiltration (3 kDa Vivaspin cutoff filter), which included four washing cycles with 0.2 mL of the reaction buffer. A similar procedure was followed for the isolation of HTrxn$(SH)_2$ after an incubation of Htrxn-S_2 with DL-dithiothreitol (DTT, 10 mM) for 20 min at room temperature. In selected experiments, separation of HTrxn derivatives from LMM compounds was achieved by size-exclusion (SE) HPLC on a Protein Pak 125 gel filtration column (0.78 cm × 30 cm; Waters, Milford, MA). HPLC-SE separations were carried out with a mobile phase consisting of 20 mM phosphate buffer (pH 7.4), 100 mM NaCl, and 0.2 mM EDTA at a flow rate of 1 mL/min. The electronic absorbance of the eluate was followed in the wavelength range of 210−400 nm with a Shimadzu (Kyoto, Japan) diode array detector.

Western Blots. Cells were disrupted by three consecutive freeze and thaw cycles and then centrifuged at 15000*g* for 15 min at 4 °C to remove membrane fractions. Equal amounts of protein (20−30 μg) were resolved by SDS−PAGE (10%) and transferred onto a nitrocellulose membrane. The membrane was blocked in 5% (w/v) dried milk powder in TBS (Tris-buffered saline) with 0.01% (v/v) Tween 20 at room temperature and incubated with anti-TrxR1 (rabbit IgG, Upstate) (1:500 dilution) overnight in 5% (w/v) BSA in TBS with 0.01% (v/v) Tween 20. Secondary antibody (HRP-conjugated anti-rabbit IgG, 1:1000; Pierce, Rockford, IL) was then added to the membrane for 1 h at room temperature. Thereafter, the membrane was washed, exposed to HRP substrate (Pierce SuperSignal West Pico Chemiluminescent Substrate), and visualized by chemiluminescence on autoradiography film.

Caspase 3 Assay. Caspase 3 activity was measured fluorometrically on an LS50B Perkin-Elmer spectrofluorimeter (λ_{ex} = 380 nm; excitation and emission slit, 5 nm) using Asp-Glu-Val-Asp-7-amido-4-methylcoumarin as a substrate (Sigma).

TrxnR Assay. TrxnR activity was determined in a coupled assay with *E. coli* Trxn (10 μM) and 5,5′-dithiobis(2-nitrobenzoic acid) (DTNB) as described in ref *35*. One unit of TrxnR activity was defined as the formation of 74 μmol of 5-mercapto-2-nitrobenzoic acid (1 absorbance unit at 412 nm; ϵ_{412} = 13 500 M^{-1} cm^{-1}) per minute per milliliter at pH 7.0 and 25 °C.

Data Analysis. Results are given as means ± the standard error (n = 3−6).

RESULTS

Trxn-Catalyzed Denitrosation of LMM RSNOs. Activated mouse macrophages and vascular smooth muscle cells have been shown to produce NO_2^- at a rate of 50−70 nmol (mg of protein)$^{-1}$ h^{-1} for up to 20 h (*36*, *37*). In cells, NO forms metal−nitrosyl complexes and N_2O_3 that can act as *S*-nitrosating agents (*38*, *39*). Since GSH is the most abundant intracellular thiol (1−5 mM or up to 100 nmol/mg of protein), formation of GSNO is expected to follow the production of endogenous NO. Indeed, GSNO has been detected in the brain (*40*) and liver (*41*) of healthy rats in amounts of 15−34 pmol/mg of protein. Upon diffusion across plasma membranes, NO can nitrosate extracellular

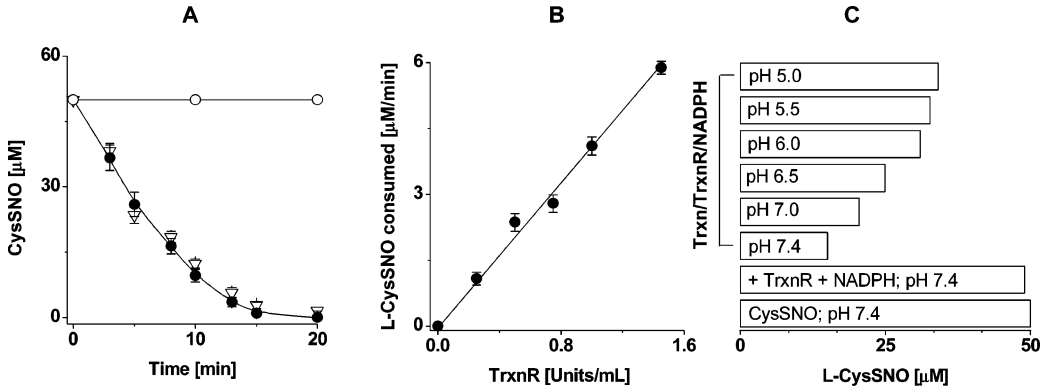

FIGURE 2: Kinetic analysis of the denitrosation of CysSNO by Trxn. All reaction conditions were as indicated in Figure 1. (A) D-CysSNO (●) and L-CysSNO (▽) with Trxn, TrxnR, and NADPH and (○) L-CysSNO with TrxnR and NADPH. (B and C) Effects of TrxnR activity and pH on the Trxn-catalyzed denitrosation of L-CysSNO (NADPH, 0.4 mM; incubation time, 10 min). The data in panels A and B are presented as mean values of three independent experiments ± the standard error.

thiols. The plasma concentrations of GSH, cysteine, and homocysteine are 2−4, 8−10, and 15−50 μM, respectively (*42*). In extracellular pulmonary fluids, the concentration of GSH is in the range of 40−400 μM (*42*), while in bile duct, the concentration of cysteine varies from 2 to 25 μM (*43*). Hence, formation of LMM RSNOs could be predicted in both the intra- and extracellular milieu, with the notions that (i) this process is efficiently catalyzed by copper ions (*44*) and (ii) extracellular CysSNO and HCysSNO (but not GSNO) can be taken up by cells via amino acid transport system L (*45*−*48*). Irrespective of the sites of nitrosation, the relatively low intracellular concentrations of RSNOs (picomoles vs nanomoles of NO_2^- per milligram of protein) can be explained with poor utilization of NO for their biosynthesis and/or efficient catabolism of this class of metabolites. To further characterize the enzyme-dependent catabolism of RSNOs, we have studied the denitrosation of CysSNO, HCysSNO, and SNAP by Trxn.

In contrast to ADH, which denitrosates specifically GSNO (*13*), Trxn catalyzed the denitrosation of all LMM RSNOs that were studied (Figure 1). Consumption of RSNOs required the presence of the complete Trxn/TrxnR/NADPH system (Figure 1B). The rate of GSNO denitrosation remained unchanged in the presence of either EDTA or desferrioxamine and under anaerobic conditions (data not shown), indicating that this process was not dependent on catalysis by transition metal ions. Maximal reaction rates were attained with 5−10 μM Trxn (Figure 1C), well within the physiological concentrations of this protein [5−50 μM (*17*, *49*)]. Initial velocities measured between the first and second minute of GSNO consumption were in good agreement with the studies of Nikitovic and Holmgren (*11*): at 0.1 μM TrxnR and 0.4 mM NADPH, υ_{max} was 1.2 nmol of GSNO (nmol of Trxn)$^{-1}$ min^{-1}. The υ_{max} values for CysSNO, HCysSNO, and SNAP were 1.2, 0.3, and 0.1 nmol of substrate (nmol of Trxn)$^{-1}$ min^{-1}, respectively (Figure 1C). In comparison, the denitrosation of GSNO by ADH and PDI and the metabolism of arginine by NOS are characterized by υ_{max} values of 2.6, 0.3, and 140 nmol of substrate (nmol of enzyme)$^{-1}$ min^{-1}, respectively (*12*, *13*, *50*). The reported K_m^{GSNO} values of Trxn, ADH, and PDI are 10, 28, and 50 μM, respectively (*11*−*13*). Recently, Liu et al. (*4*) reported a marked increase in the cellular levels of LMM and protein RSNOs, tissue damage, and mortality following endotoxic or bacterial challenge of ADH-deficient mice. However, assessment of the relative contribution of Trxn, ADH, and PDI in the catabolism of GSNO is difficult because of the different cellular and tissue compartmentalization of the three enzymes.

While it has been shown that the cardiovascular (*51*, *52*) and ventilatory (*53*) effects of CysSNO are specific to the L-isoform, suggesting the occurrence of stereospecific reactions of *trans*-S-nitrosation (*54*), we were interested in verifying whether Trxn exhibits differential activity for these stereoisomers. However, the data presented in Figure 2A indicate that the rates of Trxn-catalyzed denitrosation of L-CysSNO and D-CysSNO are identical. In contrast, the denitrosation of CysSNO was dependent on the concentration of TrxnR and the acidity of the reaction solutions (Figure 2B,C), which could be related to the steady-state concentration of Trxn$(SH)_2$ and the protonation of Trxn-Cys(32)-S^- (pK_a = 7.5), respectively.

Trxn-Dependent Denitrosation of S-Nitrosoproteins. Interactions of HTrxn(SH)$_2$ and GSH with ONS-HTrxn-S$_2$ and S-Nitrosocaspase 3. Trxn and HTrxn denitrosate GSNO at comparable rates, which suggests that their active sites contain cysteine residues with similar redox properties (*11*). However, unlike thioredoxins from lower species, mammalian thioredoxin type 1 contains additional cysteines at positions 62, 69, and 73 (*55*). Nitrosation of either cysteine 69 or 73 leads to formation of OSN-HTrxn-S_2, which has been suggested to impede apoptosis via *trans*-S-nitrosation of caspase 3 (*56*, *57*). Within the scope of this mechanism, we were interested in assessing the stability of ONS-HTrxn-S_2 in the presence of GSH and HTrxn-$(SH)_2$, respectively. Incubation of human thioredoxin with an oxidized active site (HTrxn-S_2, 0.4 mM; three SH functions per mole of HTrxn-S_2, as assessed by the DTNB assay; data not shown) with GSNO (2 mM) for 30 min at room temperature resulted in the nitrosation of a single thiol on HTrxn to give ONS-HTrxn-S_2, as previously reported (*57*, *58*). In parallel, reduction of HTrxn-S_2 (0.4 mM) with DTT (10 mM) resulted in the formation of HTrxn[$Cys_{(32/35)}SH]_2$. Separation of HTrxn from DTT and GSNO was carried out either via ultrafiltration or by HPLC-SE as described in Experimental Procedures. In the presence of Trxn$(SH)_2$, ONS-HTrxn-S_2 was consumed in a second-order type 2A → product reaction ($d[A]_t/dt = -k[A]^2$), for which a plot of $1/[A]_t$ against time yielded a straight line with positive slope (k) of 309 M^{-1} s^{-1} (Figure 3A). An excess of 6 molar equiv of Trxn$(SH)_2$

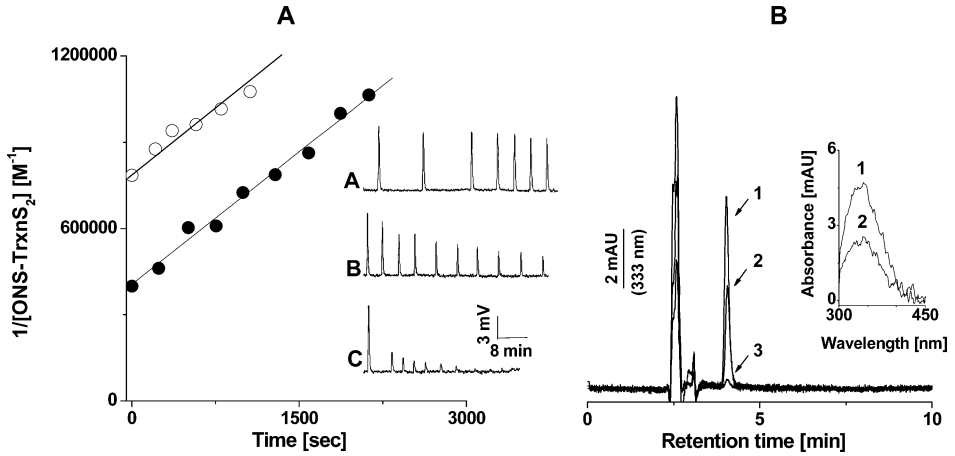

FIGURE 3: Both HTrxn(SH)$_2$ and GSH denitrosate ONS-HTrxn-S$_2$. (A) HTrxn-(SH)$_2$ [(○) 1.5 and (●) 15 μM] and ONS-HTrxn-S$_2$ [(○) 1.5 and (●) 2.5 μM] were incubated at 37 °C in 0.1 M phosphate buffer (pH 7.4) containing 0.2 mM EDTA. At given time points, aliquots from the reaction solution were assessed for ONS-HTrxn-S$_2$ content. The inset shows the spectra for 2.5 μM OSN-HTrxn-S$_2$ in the absence (A) and presence (B) of 15 μM HTrxn(SH)$_2$ and (C) in the presence of 0.5 μM *S*-nitrosocaspase 3, 5 μM HTrxn, 1 unit/mL rat liver TrxnR, and 0.2 mM NADPH. (B) HPLC−UV profiles of solutions containing ONS-HTrxn-S$_2$ and GSH. ONS-HTrxn-S$_2$ (50 μM) was incubated at 20 °C in 0.1 M phosphate buffer (pH 7.4) containing 0.2 mM EDTA in the absence (chromatogram 3) and presence of GSH (5 mM, chromatogram 1). Chromatogram 2 is for a standard solution of GSNO (25 μM). In the inset, tracings 1 and 2 represent the electronic spectra of the compounds eluted under peaks 1 and 2, respectively. The maximum at 334 nm was attributed to the absorption of the SNO function of GSNO.

did not change the kinetic profile to a pseudo-first-order reaction (Figure 3A), for which a plot of $\ln([A]_0/[A]_t)$ against time would yield a straight line with a negative slope of k. Under similar reaction conditions, GSH readily denitrosated ONS-HTrxn-S$_2$ (Figure 3B). The reaction proceeded with a quantitative transfer of the NO function, whereby 50 nmol of ONS-Cys-HTrxn-S$_2$ generated an equimolar amount of GSNO within 10 min of incubation at room temperature. The identity of GSNO formed via transfer of the NO function from ONS-HTrxn-S$_2$ to GSH was confirmed by HPLC analysis on C-18 matrix, whereby the retention times of the experimental peaks were compared with that of GSNO from a standard solution (Figure 3B; peaks 1 and 2, respectively). Further identification was carried out by comparison of the electronic spectra of the compounds eluted under peaks 1 and 2 (Figure 3B, inset). Under these chromatographic conditions, both ONS-HTrxn-S$_2$ and HTrxn-S$_2$ eluted with the front of the solvent (retention time, 2.4 min).

Similar to *E. coli* Trxn (*7*), the complete HTrxn/TrxnR/NADPH system readily denitrosated *S*-nitrosocaspase 3 (Figure 3A, inset C). In the absence of HTrxn, *S*-nitrosocaspase did not decompose to any significant extent (data not shown). These results suggest that both *S*-nitrosocaspase 3 and ONS-HTrxn-S$_2$, if formed in cells, will undergo HTrxn/TrxnR/NADPH-dependent denitrosation. The denitrosation of ONS-HTrxn-S$_2$ would be regulated by GSH, as well.

Effects of TrxnR on the Nitrosative Inactivation of Caspase 3 in HepG2 Cells. To assess the effects of the HTrxn/TrxnR system on the nitrosative inactivation of caspase 3, experiments were carried out with control and TrxnR-deficient HepG2 cells. In contrast to hepatocytes, HepG2 cells are deficient in some phase I enzymes, including ADH (*59*−*61*). In cells, TrxnR was silenced using either siRNA or ANF, while activation of caspase 3 was attained with paclitaxel with NU6140 and TNF-α with cycloheximide, respectively.

Both siRNA (30 nM; incubation time, 72 h) and ANF (5 μM; incubation time, 12 h) caused an ∼50% decrease in the activity of TrxnR (Figure 4A) without affecting the levels of intracellular GSH to any significant extent (data not shown). Western blot analysis established that, in siRNA-treated cells, the protein levels of TrxnR had markedly decreased (Figure 4A, inset). For *S*-nitrosation of thiols, cells were incubated with SNCEE, a membrane-permeable compound that was shown to *trans*-S-nitrosate proteins in a number of cell types (*7*, *26*, *62*, *63*). While 0.2−0.8 mM SNCEE caused cytotoxicity with concomitant inhibition of TrxnR (Figure 4B,C), further experiments that aimed to assess the nitrosative inactivation of caspase 3 in HepG2 cells were carried out with 50 μM SNCEE.

Figure 5A (spectral series 1) depicts the kinetics of formation of 7-amino-4-methylcoumarin in lysates of TNF-α-treated HepG2 cells containing Ac-Asp-Glu-Val-Asp-7-amido-4-methylcoumarin as a substrate of caspase 3. In this process, the requirement for caspase 3 catalysis was suggested by the inhibitory effects of 5-[(*S*)-(+)-2-(methoxymethyl)pyrrolidino]sulfonylisatin (MSF) (Figure 5A, spectral series 2) and SNCEE [Figure 5B (*7*)], as well as by the reconstitution of the enzymatic activity by DL-dithiothreitol (DTT) after SNCEE treatment (Figure 5B); DTT has been shown to readily denitrosate *S*-nitrosocaspase 3 (*7*, *64*, *65*).

In previous experiments with human neutrophils, we have observed that steady-state concentrations of intracellular *S*-nitrosothiols could be reached after an incubation of the cells with 0.1 mM SNCEE for 5−10 min (*26*). Hence, control and TrxnR-deficient HepG2 cells were incubated for 15 min with 50 μM SNCEE. These cells were then washed with PBS, and the activity of caspase 3 was assessed either immediately (time for preparation of cell lysates, 5 min) or after an additional incubation for 35 min at 37 °C. The rationale for this experimental design was based on the kinetics of denitrosation of RSNOs by the (H)Trxn/TrxnR/NADPH system (Figures 1−3), with the hypothesis that time-dependent increases in caspase 3 activity would reflect the rates of endogenous denitrosation of *S*-nitrosocaspase 3. Treatment of control HepG2 cells with SNCEE led to ∼80%

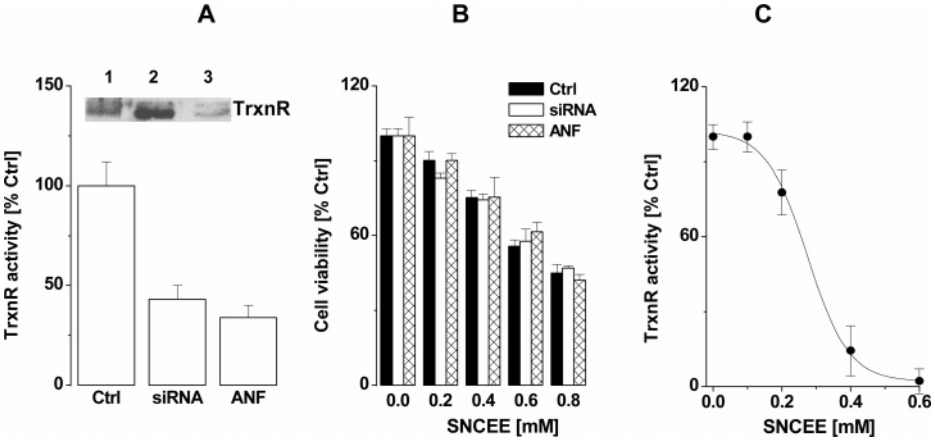

FIGURE 4: ANF, siRNA, and SNCEE impede the activity of TrxnR in HepG2 cells. (A) Experiments aimed at silencing TrxnR in HepG2 cells with siRNA and ANF were carried out as described in Experimental Procedures. The inset shows the Western analysis of cells transfected with scrambled siRNA (lane 1), untransfected cells (lane 2), and siRNA-transfected cells (lane 3). (B) Toxicity of SNCEE in control and siRNA- and ANF-pretreated HepG2 cells. (C) TrxnR activity in HepG2 cells treated with SNCEE. The control activity of TrxnR is 0.12 unit/mg of protein. The results represent the mean ± the standard error ($n = 4$).

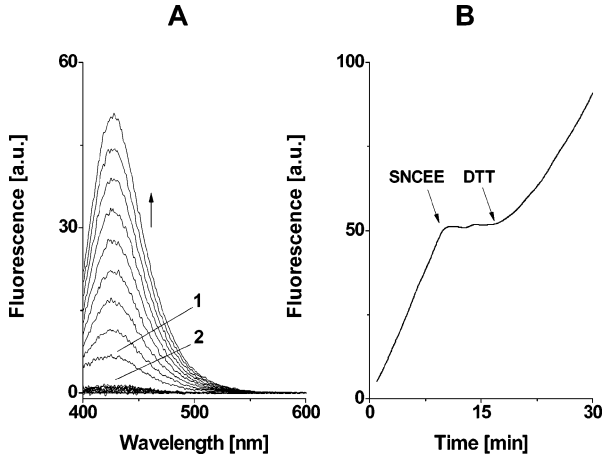

FIGURE 5: SNCEE inhibits caspase 3 in lysates of HepG2 cells. Reactions were carried out at 20 °C in 0.1 M phosphate buffer containing EDTA (0.1 mM), lysates from (TNF-α and cycloheximide)-treated HepG2 cells (0.024 mg of protein/mL), and Ac-Asp-Glu-Val-Asp-7-amido-4-methylcoumarin (0.1 mM) as a substrate of caspase 3. (A) Formation of 7-amino-4-methylcoumarin in the absence (spectral series 1) and presence of the caspase 3 inhibitor MSF (50 μM; spectral series 2). The time interval between two consecutive scannings was 1 min; an arrow indicates the direction of the spectral changes. (B) Effects of SNCEE (50 μM) and DTT (5 mM) on the formation of 7-amino-4-methylcoumarin. In lysates of nontreated and treated (TNF-α plus cycloheximide) HepG2 cells, 7-amino-4-methylcoumarin was generated at rates of 0.1 and 2.8 nmol min^{-1} (mg of protein)$^{-1}$ mL^{-1}, respectively.

(5 min) and 20% (35 min) inhibition of caspase 3, whereby DTT accelerated the reconstitution of the enzymatic activity (Figure 6A). In contrast, the regeneration of caspase 3 activity was insignificant in TrxnR-deficient cells, which suggests the requirement for HTrxn catalysis in this process. In these experiments, deletion of TrxnR and induction of caspase 3 were achieved with siRNA and paclitaxel, respectively. Qualitatively similar results were obtained when inhibition of TrxnR and induction of caspase 3 were carried out with ANF and TNF-α, respectively (Figure 6B).

Trxn-Catalyzed Denitrosation of HepG2 Cell-Derived S-Nitrosoproteins. We further tested the ability of Trxn to denitrosate a complex mixture of *S*-nitrosoproteins. To this end, proteins (molecular masses of >10 kDa) were isolated from HepG2 cells and subjected to *S*-nitrosation as described

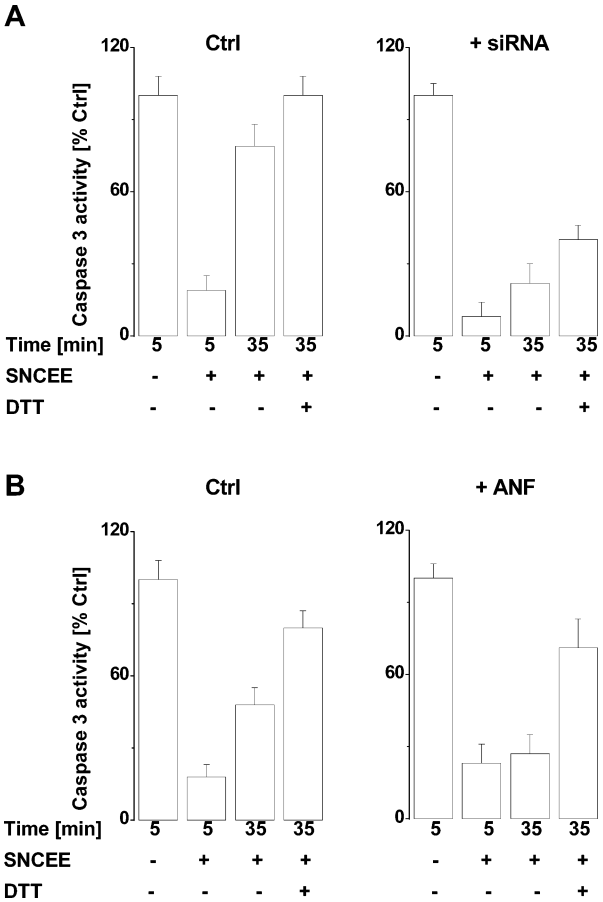

FIGURE 6: SNCEE and TrxnR modulate the activity of caspase 3 in HepG2. Cells were rendered TrxnR-deficient by treatment with siRNA (A) or ANF (B); then, caspase 3 activity was stimulated with either paclitaxel and NU6140 (A) or TNF-α and cycloheximide (B) as described in Experimental Procedures. After being incubated for 15 min at 37 °C with SNCEE (50 μM), the cells were washed with PBS, and caspase 3 activity was assessed at the indicated times in the absence or presence of DTT (5 mM). In control lysates of HepG2 cells, the rate of generation of 7-amino-4-methylcoumarin was 0.7 nmol min^{-1} (mg of protein)$^{-1}$ mL^{-1} (A) and 2.7 nmol min^{-1} (mg of protein)$^{-1}$ mL^{-1} (B). The results represent the mean ± the standard error ($n = 3$).

in Experimental Procedures. The complete Trxn/TrxnR/NADPH system caused only a partial denitrosation of HepG2

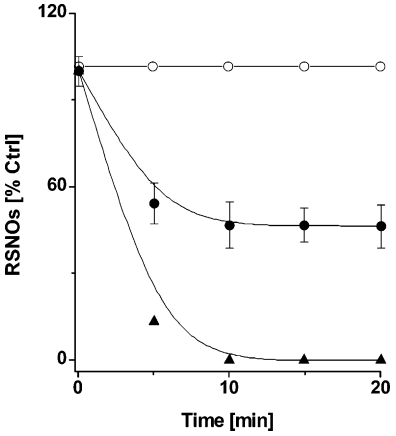

FIGURE 7: Trxn catalyzes the denitrosation of HepG2 cell-derived *S*-nitrosoproteins. Reactions were carried out at 37 °C in 0.1 M phosphate buffer (pH 7.4) containing HepG2 cell-derived *S*-nitrosoproteins (1 mg of protein/mL; 23.85 nmol of RSNOs/mg of protein; molecular mass of >10 kDa), TrxnR (0.08 μM, 1 unit/mL), and NADPH (0.2 mM) in the absence (○) and presence (●) of Trxn (5 μM). (▲) HepG2 cell-derived *S*-nitrosoproteins with DTT (10 mM).

cell-derived *S*-nitrosoproteins (Figure 7). However, DTT (10 mM) fully denitrosated the protein extract, which suggests that the reaction solution contained *S*-nitrosoproteins that were not substrates of Trxn. To verify whether Trxn exerts higher activity toward selected groups of proteins, the GSNO-treated cell extract containing *S*-nitrosoproteins was separated by HPLC-SE. *S*-Nitrosoproteins were grouped by molecular mass via elution through an SE Protein-Pak 125 column, which can resolve proteins with molecular masses of 2−80 kDa and can distinguish proteins differing by 15% in molecular mass. In control experiments, a retention time−molecular mass relationship was established via separation of standard solutions of cytochrome *c*, myoglobin, superoxide dismutase, and albumin [molecular masses of 12.2, 18.8, 31, and 66 kDa, respectively (Figure 8A, peaks a−d, and Figure 8B)]. Under these chromatographic conditions, proteins exhibited t_R values of 5−10 min while LMM compounds (including GSNO) eluted with a t_R of 12.4 min.

In chromatographic separations of control and GSNO-treated proteins (0.1 mg on the column; Figure 8A), the first 5 mL of the eluate was discarded; then, 10 consecutive fractions of 0.5 mL were collected and assessed for thiols, proteins, and RSNOs (Figure 8C−F). In the fractions that were collected, the mass distribution of proteins followed the sequence 1−4 > 7−10 ≫ 5 and 6 (Figure 8C). Treatment of fractions 3−6 with Trxn, TrxnR, and NADPH resulted in either partial or complete denitrosation of RSNOs (Figure 9A). *S*-Denitrosation of proteins was not observed if either Trxn or TrxnR was omitted from the reaction system. Marked GSNO- and Trxn-dependent S-nitrosation and denitrosation, respectively, were observed for fractions enriched with 23−40 kDa proteins (Figures 6A and 8F). Interestingly, these fractions had the lowest protein content but were particularly rich in thiols (Figure 8E). Furthermore, all RSNOs in fraction 6 were denitrosated by Trxn (Figure 9A). The substrate specificity of Trxn toward *S*-nitrosoproteins with a molecular mass of <30 kDa is further supported by the data presented in Figure 9B; RhoA(SNO)$_6$ (~27 kDa; prepared as described in Experimental Procedures) was readily denitrosated by the complete Trxn/TrxnR/NADPH system (Figure 9B2), whereas

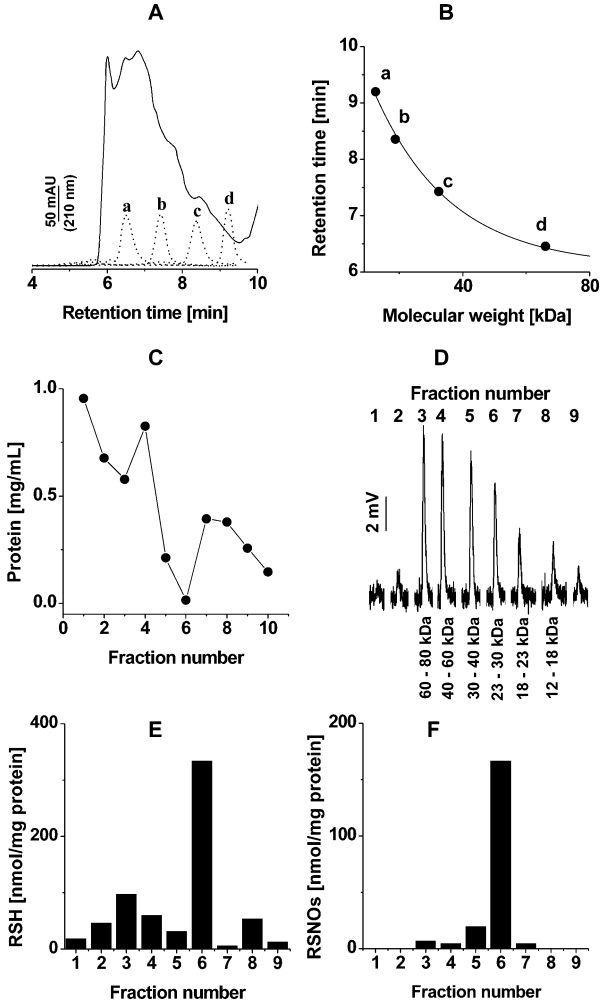

FIGURE 8: HPLC-SE analysis of HepG2 cell-derived *S*-nitrosoproteins. Proteins with a molecular mass of >10 kDa (5 mg/mL) were isolated from lysates of HepG2 cells and then treated with GSNO (0.3 mM) for 30 min at 20 °C. The final reaction solution was separated by HPLC-SE on a Protein Pak 125 column into fractions (0.5 mL; 5−10 min) of groups of proteins within a specific molecular mass range [A (—)]. The retention time−molecular mass relationship for the column used was assessed by separation of bovine albumin [0.25 μM (a)], SOD [1 μM (b)], myoglobin [1 μM (c)], and Cc [5 μM (d)] (•••). (B−F) Content of proteins, RSH, and RSNOs in the fractions collected. Differences in the data obtained from two independent experiments did not exceed 5%.

omission of Trxn from the reaction milieu impeded the process (Figure 9B1).

DISCUSSION

In this work, experimental evidence that Trxn catalyzes the denitrosation of LMM and protein RSNOs in model systems and in HepG2 cells is presented. Notably, all HepG2 cell-derived *S*-nitrosoproteins with a molecular mass of 23−30 kDa were substrates of Trxn.

The reduction of LMM disulfides and RSNOs by Trxn could be explained with the general mechanisms of cyclic disulfide−dithiol-type and RSNO−dithiol-type interactions, which are described by either a simple S_N2 process or addition−elimination interactions (*5*, *66*−*68*). Strained cyclic disulfides are reduced at higher rates, whereby a Brønsted relationship is followed in the values of pK_a of both the nucleophilic thiol and of the thiol being displaced (*69*, *70*). The redox-active SS bridge in Trxn is surrounded by a

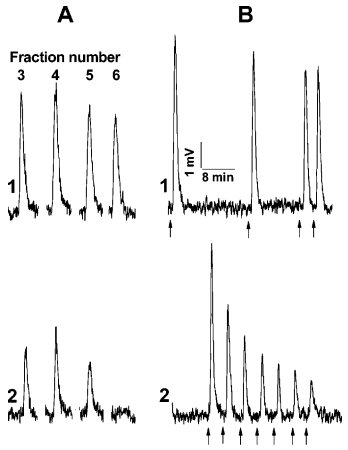

FIGURE 9: Trxn-catalyzed denitrosation of HepG2 cell-derived *S*-nitrosoproteins and RhoA(SNO)$_6$. (A) HPLC-SE fractions containing *S*-nitrosoproteins were collected as described in the legend of Figure 5 and then incubated at 37 °C for 30 min with TrxnR (0.08 μM) and NADPH (0.2 mM) in the absence (1) and presence (2) of Trxn (10 μM). (B) RhoA(SNO)$_6$ (18 μM; prepared as described in Experimental Procedures) was incubated at 37 °C with TrxnR (0.08 μM) and NADPH (0.2 mM) in the absence (1) and presence (2) of Trxn (5 μM). At given time points (arrows), aliquots from the reaction solutions were assessed for RSNO content as described in Experimental Procedures. The data presented are representative of two independent experiments.

hydrophobic molecular surface that is believed to represent the area involved in binding to TrxnR (*16*), while cysteine 32, located in the active site of Trxn(SH)$_2$, exhibits a pK_a of 7.5 (*71*, *72*). Since most biological thiols have pK_a values of 8−11, the reduction of their SS and/or SNO functions by Trxn-cysteine 32 would be kinetically favorable. If rate differences on the order of a factor of 2 may be considered to be important, it could be concluded that Trxn denitrosates CysSNO, HCysSNO, SNAP, and GSNO without any significant substrate selectivity. Cysteine, homocysteine, GSH, and *N*-acetylpenicillamine are thiols with pK_a values of 8.33, 8.87, 9.12, and 9.65, respectively (*67*), while the relatively slower denitrosation of SNAP could be explained with the inductive and steric effects of the two methyl groups in the vicinity of the SNO function. However, these mechanistic considerations have limited predictive value for the identification of *S*-nitrosoproteins as substrates of Trxn. Depending on their microenvironment, protein thiols exhibit pK_a values of 4−11. Recently, Stamler et al. (*73*) proposed a consensus sequence for protein *S*-nitrosation. On the other hand, on the basis of the analysis of the three-dimensional (3D) structures of several known proteins, Ascenzi et al. (*74*) concluded that the microenvironment of a NO-reactive cysteine residue is more important for reactions of *S*-(de)-nitrosation than the presence of a specific amino acid sequence. To date, structural data for more than 18 000 proteins have been deposited in the Human Protein Reference Database,[2] where 1733 proteins with molecular masses of 23−30 kDa are found. Most of these proteins contain thiol functions that could be converted to *S*-nitrosothiols by NO derivatives. Nevertheless, the generation of structure−activity relationship (SAR)-based hypotheses that can be used to predict the activity of Trxn toward SS and/or SNO functions in proteins has proven to be difficult, in part due to the insufficient data on the p$K_{a(SH)}$ values of most proteins and the accessibility of their SNO functions. While extensive X-ray studies have elucidated the 3D structure of many proteins, only a handful of reports have pointed to the occurrence of considerable conformational changes upon protein *S*-nitrosation (*75*, *76*).

Although empirical, the data presented in Figure 6A provide a foundation for analysis and prediction of the effects of NO on thiol-containing proteins in cells. It is tempting to speculate that *S*-nitrosoproteins that are not substrates of Trxn will have higher intracellular concentrations. In contrast, inhibition of the Trxn/TrxnR system may lead to increased concentrations of *S*-nitrosoproteins with molecular masses in the range of 23−30 kDa. This hypothesis is in agreement with the studies of Lopez-Sanchez et al. (*77*), who observed that in hepatocytes proteins with molecular masses of <30 kDa are particularly resistant to *S*-nitrosation. It could be further hypothesized that LMM disulfide mimics of Trxn, such as lipoic acid (LA), will minimize the impact of nitrosative stress. In cells, TrxnR, GSH reductase, and lipoamide dehydrogenase catalyze the reduction of LA to dihydrolipoic acid, which readily denitrosates LMM and protein RSNOs (*7*). Examples of thiol-containing proteins with molecular masses of 23−30 kDa that can undergo *S*-nitrosation in biological systems are the members of the GTPase family [including Ran(SH)$_3$, Ras(SH)$_4$, RhoA(SH)$_6$, and ERas(SH)$_8$], calpain(SH)$_3$ (small subunit 1), and the carbonic anhydrase(SH)$_4$ (*78*−*80*). While Trxn has been shown to regenerate critical thiols in some of these proteins via reduction of S−S bonds (*81*−*83*), denitrosation of their *S*-nitrosoderivatives has not been reported thus far. The data presented in Figure 9B indicate that Trxn catalyzes the denitrosation of RhoA(SNO)$_6$ (*84*), while SNCEE impeded the activity of RhoA more efficiently in TrxnR-deficient HepG2 cells (R. Sengupta, B. Zuckerbraun, E. Tzeng, T. Billiar, and D. Stoyanovsky, data not shown).

In recent years, the *S*-nitrosation of HTrxn-S$_2$ in side cysteines 62, 69, and 73 has been the focus of considerable interest. Haendeler et al. (*56*) reported that overexpression of HTrxn in endothelial cells activates eNOS, increases basal levels of endogenous RSNOs, and inhibits TNF-α-induced apoptosis. Experiments with genetically manipulated cells that express cysteine 69-lacking Trxn suggested that these effects may reflect HTrxn nitrosation in its redox-inactive cysteine 69 to ONS-Cys$_{(69)}$-HTrxn-S$_2$, which, in turn, *trans*-*S*-nitrosates activators of apoptosis (*56*). In chemical systems, Mitchell and Marletta found that GSNO preferentially nitrosates cysteine 73 to form ONS-Cys$_{(73)}$-HTrxn-S$_2$ without affecting cysteine 69, whereas Weichsel et al. reported that, at physiological pH, only cysteine 62 could be *S*-nitrosated by GSNO [from 50 μM to 15 mM (*58*)]. Experimental variables that may affect the regioselectivity of the *trans*-*S*-nitrosation of HTrxn-S$_2$ have been discussed in ref *58*. In neutral solutions of HTrxn-S$_2$ (10 μM), GSNO (50 μM), and GSH (1 mM), Weichsel et al. (*58*) observed ∼30% conversion of HTrxn-S$_2$ to ONS-Cys$_{(62)}$-HTrxn-S$_2$. In contrast, the yield of ONS-Cys$_{(62)}$-HTrxn-S$_2$ was quantitative in the absence of GSH, which indicates that the nitrosation process could be described by a GSH-dependent equilibrium that may be shifted in favor of HTrxn-S$_2$ at physiological (nanomolar) concentrations of GSNO. On the other hand, Mitchell and Marletta reported that ONS-Cys$_{(73)}$-HTrxn-S$_2$ *trans*-S-nitro-

[2] At www.hprd.org.

sates caspase 3 to ONS-$Cys_{(163)}$-caspase 3 at a rate of 196 M^{-1} s^{-1}, thus suggesting a specific pathway for NO-dependent inactivation of caspase 3 in apoptotic cells (*57*). It is noteworthy that *S*-nitrosocaspase 3 is relatively stable in the presence of 5−10 mM GSH (*85*). However, the data presented in Figure 3 indicate that in cells both GSH and $HTrxn-(SH)_2$ ($k = 309$ M^{-1} s^{-1}) will compete with caspase 3 for ONS-$HTrxn-S_2$, if formed to any significant extent. While the cytosolic concentrations of HTrxn and GSH are orders of magnitude higher than these of caspase 3 (*17*, *49*, *86*), it is likely that the denitrosation of ONS-$HTrxn-S_2$ by GSH and $HTrxn(SH)_2$ will be the dominant processes. In parallel, *S*-nitrosocaspase would be denitrosated by the complete HTrxn/TrxnR/NADPH system. Supporting this hypothesis are the data presented in Figures 3A (inset C) and 6. While the *S*-nitrosative inactivation of caspase 3 by both exogenous and endogenous NO is a well-established phenomenon, the data obtained indicate that the HTrxn/TrxnR/NADPH system in HepG2 cells tends to maintain this protease in a reduced, SH state. It could be further hypothesized that shifts in the rates of *S*-nitrosation and denitrosation of caspase 3 following changes in either NO production or activity of the HTrxn/TrxnR/NADPH system would dictate whether cells will undergo apoptosis (caspase 3-SH) versus necrosis (caspase 3-SNO). Pathological states that are characterized by a sustained production of NO and increased levels of RSNOs include inflammation (*4*, *87*), neurodegenerative disorders (*88*), and biliary cirrhosis (*89*). Recently, Grattagliano et al. (*87*) reported that cholestasis is associated with significant changes in hepatic Trxn and RSNOs, whereby Trxn was found to be inversely related to the levels of RSNOs.

In the presence of TrxnR and NADPH, the denitrosation of RSNOs by catalytic amounts of both Trxn and HTrxn suggests that these isozymes initially undergo *trans*-*S*-nitrosation in their low-pK_a thiol of cysteine 32 (**1**; Scheme 1). Due to the presence of a vicinal thiol group (cysteine 35), **1** undergoes a rapid ring closure to disulfide **3** with concomitant release of nitroxyl (HNO), the one-electron reduction product of NO (*7*). In turn, **3** may be reduced back to **1** or, competitively, may undergo *S*-nitrosation at cysteine 62, 69, or 73 to form **4**. In GSH- and TrxnR-deficient cells, **4** may reach steady-state concentrations that are sufficient for *trans*-S-nitrosation of other cellular proteins, including caspase 3. This mechanism is particularly interesting with regard to the possibility of a substrate-specific *trans*-*S*-nitrosation via protein−protein interactions. However, further studies are needed to understand the reactions that lead to formation of **4** as well as to elucidate its fate in complex biological matrices.

The catalytic cycle presented in Scheme 1 further suggests that NO could be converted to HNO via the intermediate formation of RSNOs. In contrast to NO, HNO readily interacts with thiols to form disulfides and hydroxylamine (*90*). The rate constant for the interaction of GSH and HNO has been reported to be 1×10^5 to 2×10^{-6} M^{-1} s^{-1} (*91*, *92*), which suggests that HNO generated within cells would be predominantly scavenged by GSH. Nevertheless, competitive interactions of HNO with cellular proteins containing low-pK_a thiols which are deprotonated at physiological pH and/or metal complexes (*90*, *93*, *94*) cannot be ruled out. Exogenous HNO has been shown to exert multifaceted pharmacological effects. HNO has been found to be a metabolite of the alcohol deterrent agent cyanamide (*95*), to be a potent dilator of rat coronary vasculature (*96*), to exert cardiotoxic and cardioprotective properties in models of myocardial ischemia and reperfusion injury (*97*) and of heart failure (*98*), respectively, to exert increased toxicity in acidic cells (*99*) and to impede tumor growth in mice (*100*), and to mediate the in vitro activation potassium (*96*) and calcium channels (*100*, *101*). However, further studies are needed to better understand the biosynthesis and Trxn-dependent catabolism of RSNOs in intact cells, as well as to depict the concomitant biochemistry of HNO.

Scheme 1

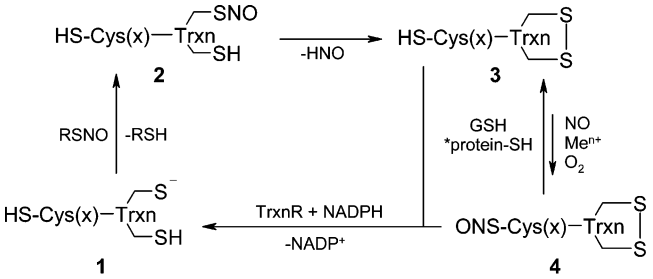

*Including **1** and caspase 3; Me^{n+}, transition metal ions; Cys(x), cysteine 62, 69 or 73

REFERENCES

1. Tannenbaum, S. R., and White, F. M. (2006) Regulation and specificity of S-nitrosylation and denitrosylation, *ACS Chem. Biol. 1*, 615−618.
2. Chung, K. K., Dawson, T. M., and Dawson, V. L. (2005) Nitric oxide, S-nitrosylation and neurodegeneration, *Cell. Mol. Biol. (Paris, Fr., Print) 51*, 247−254.
3. Scatena, R., Bottoni, P., Martorana, G. E., and Giardina, B. (2005) Nitric oxide donor drugs: An update on pathophysiology and therapeutic potential, *Expert Opin. Invest. Drugs 14*, 835−846.
4. Liu, L., Yan, Y., Zeng, M., Zhang, J., Hanes, M. A., Ahearn, G., McMahon, T. J., Dickfeld, T., Marshall, H. E., Que, L. G., and Stamler, J. S. (2004) Essential roles of S-nitrosothiols in vascular homeostasis and endotoxic shock, *Cell 116*, 617−628.
5. Arnelle, D. R., and Stamler, J. S. (1995) NO^+, NO, and NO^- donation by S-nitrosothiols: Implications for regulation of physiological functions by S-nitrosylation and acceleration of disulfide formation, *Arch. Biochem. Biophys. 318*, 279−285.
6. Lei, S. Z., Pan, Z. H., Aggarwal, S. K., Chen, H. S., Hartman, J., Sucher, N. J., and Lipton, S. A. (1992) Effect of nitric oxide production on the redox modulatory site of the NMDA receptor-channel complex, *Neuron 8*, 1087−1099.
7. Stoyanovsky, D. A., Tyurina, Y. Y., Tyurin, V. A., Anand, D., Mandavia, D. N., Gius, D., Ivanova, J., Pitt, B., Billiar, T. R., and Kagan, V. E. (2005) Thioredoxin and lipoic acid catalyze the denitrosation of low molecular weight and protein S-nitrosothiols, *J. Am. Chem. Soc. 127*, 15815−15823.
8. Petit, C., Hoffmann, P., Souchard, J. P., Nepveu, F., and Labidalle, S. (1996) [Thionitrites as potent donors of nitric oxide: Example of S-nitroso- and S,S′-dinitroso-dihydrolipoic acids], *C. R. Seances Soc. Biol. Ses Fil. 190*, 641−650.
9. Lipton, S. A., Choi, Y. B., Sucher, N. J., and Chen, H. S. (1998) Neuroprotective versus neurodestructive effects of NO-related species, *Biofactors 8*, 33−40.
10. Stamler, J. S., Simon, D. I., Osborne, J. A., Mullins, M. E., Jaraki, O., Michel, T., Singel, D. J., and Loscalzo, J. (1992) S-Nitrosylation of proteins with nitric oxide: Synthesis and characterization of biologically active compounds, *Proc. Natl. Acad. Sci. U.S.A. 89*, 444−448.
11. Nikitovic, D., and Holmgren, A. (1996) S-Nitrosoglutathione is cleaved by the thioredoxin system with liberation of glutathione and redox regulating nitric oxide, *J. Biol. Chem. 271*, 19180−19185.

12. Sliskovic, I., Raturi, A., and Mutus, B. (2005) Characterization of the S-denitrosation activity of protein disulfide isomerase, *J. Biol. Chem. 280*, 8733−8741.
13. Jensen, D. E., Belka, G. K., and Du Bois, G. C. (1998) S-Nitrosoglutathione is a substrate for rat alcohol dehydrogenase class III isoenzyme, *Biochem. J. 331* (Part 2), 659−668.
14. Uehara, T., Nakamura, T., Yao, D., Shi, Z. Q., Gu, Z., Ma, Y., Masliah, E., Nomura, Y., and Lipton, S. A. (2006) S-Nitrosylated protein-disulphide isomerase links protein misfolding to neurodegeneration, *Nature 441*, 513−517.
15. Benhar, M., Forrester, M. T., and Stamler, J. S. (2006) Nitrosative stress in the ER: A new role for S-nitrosylation in neurodegenerative diseases, *ACS Chem. Biol. 1*, 355−358.
16. Holmgren, A. (1985) Thioredoxin, *Annu. Rev. Biochem. 54*, 237−271.
17. Holmgren, A., and Bjornstedt, M. (1995) Thioredoxin and thioredoxin reductase, *Methods Enzymol. 252*, 199−208.
18. Laurent, T. C., Moore, E. C., and Reichard, P. (1964) Enzymatic Synthesis of Deoxyribonucleotides. IV. Isolation and Characterization of Thioredoxin, the Hydrogen Donor from *Escherichia coli* B, *J. Biol. Chem. 239*, 3436−3444.
19. Follmann, H., and Haberlein, I. (1995) Thioredoxins: Universal, yet specific thiol-disulfide redox cofactors, *Biofactors 5*, 147−156.
20. Goldman, R., Stoyanovsky, D. A., Day, B. W., and Kagan, V. E. (1995) Reduction of phenoxyl radicals by thioredoxin results in selective oxidation of its SH-groups to disulfides. An antioxidant function of thioredoxin, *Biochemistry 34*, 4765−4772.
21. Nordberg, J., and Arner, E. S. (2001) Reactive oxygen species, antioxidants, and the mammalian thioredoxin system, *Free Radical Biol. Med. 31*, 1287−1312.
22. Matsui, M., Oshima, M., Oshima, H., Takaku, K., Maruyama, T., Yodoi, J., and Taketo, M. M. (1996) Early embryonic lethality caused by targeted disruption of the mouse thioredoxin gene, *Dev. Biol. 178*, 179−185.
23. Nonn, L., Williams, R. R., Erickson, R. P., and Powis, G. (2003) The absence of mitochondrial thioredoxin 2 causes massive apoptosis, exencephaly, and early embryonic lethality in homozygous mice, *Mol. Cell. Biol. 23*, 916−922.
24. Wong, J. H., Cai, N., Balmer, Y., Tanaka, C. K., Vensel, W. H., Hurkman, W. J., and Buchanan, B. B. (2004) Thioredoxin targets of developing wheat seeds identified by complementary proteomic approaches, *Phytochemistry 65*, 1629−1640.
25. Kumar, J. K., Tabor, S., and Richardson, C. C. (2004) Proteomic analysis of thioredoxin-targeted proteins in *Escherichia coli*, *Proc. Natl. Acad. Sci. U.S.A. 101*, 3759−3764.
26. Clancy, R., Cederbaum, A. I., and Stoyanovsky, D. A. (2001) Preparation and properties of S-nitroso-L-cysteine ethyl ester, an intracellular nitrosating agent, *J. Med. Chem. 44*, 2035−2038.
27. Stamler, J. S., Osborne, J. A., Jaraki, O., Rabbani, L. E., Mullins, M., Singel, D., and Kloscalzo, J. (1993) Adverse vascular effects of homocysteine are modulated by endothelium-derived relaxing factor and related oxides of nitrogen, *J. Clin. Invest. 91*, 308−318.
28. Menon, N. K., Patricza, J., Binder, T., and Bing, R. J. (1991) Reduction of biological effluents in purge and trap micro reaction vessels and detection of endothelium-derived nitric oxide (edno) by chemiluminescence, *J. Mol. Cell. Cardiol. 23*, 389−393.
29. Eyer, P., and Podhradsky, D. (1986) Evaluation of the micromethod for determination of glutathione using enzymatic cycling and Ellman's reagent, *Anal. Biochem. 153*, 57−66.
30. Pennati, M., Campbell, A. J., Curto, M., Binda, M., Cheng, Y., Wang, L. Z., Curtin, N., Golding, B. T., Griffin, R. J., Hardcastle, I. R., Henderson, A., Zaffaroni, N., and Newell, D. R. (2005) Potentiation of paclitaxel-induced apoptosis by the novel cyclin-dependent kinase inhibitor NU6140: A possible role for survivin down-regulation, *Mol. Cancer Ther. 4*, 1328−1337.
31. Pastorino, J. G., and Hoek, J. B. (2000) Ethanol potentiates tumor necrosis factor-α cytotoxicity in hepatoma cells and primary rat hepatocytes by promoting induction of the mitochondrial permeability transition, *Hepatology 31*, 1141−1152.
32. Flick, D. A., and Gifford, G. E. (1984) Comparison of in vitro cell cytotoxic assays for tumor necrosis factor, *J. Immunol. Methods 68*, 167−175.
33. Altschul, S. F., Gish, W., Miller, W., Myers, E. W., and Lipman, D. J. (1990) Basic local alignment search tool, *J. Mol. Biol. 215*, 403−410.
34. Cassidy, P. B., Edes, K., Nelson, C. C., Parsawar, K., Fitzpatrick, F. A., and Moos, P. J. (2006) Thioredoxin reductase is required for the inactivation of tumor suppressor p53 and for apoptosis induced by endogenous electrophiles, *Carcinogenesis 27*, 2538−2549.
35. Karimpour, S., Lou, J., Lin, L. L., Rene, L. M., Lagunas, L., Ma, X., Karra, S., Bradbury, C. M., Markovina, S., Goswami, P. C., Spitz, D. R., Hirota, K., Kalvakolanu, D. V., Yodoi, J., and Gius, D. (2002) Thioredoxin reductase regulates AP-1 activity as well as thioredoxin nuclear localization via active cysteines in response to ionizing radiation, *Oncogene 21*, 6317−6327.
36. Vodovotz, Y., Kwon, N. S., Pospischil, M., Manning, J., Paik, J., and Nathan, C. (1994) Inactivation of nitric oxide synthase after prolonged incubation of mouse macrophages with IFN-γ and bacterial lipopolysaccharide, *J. Immunol. 152*, 4110−4118.
37. Bani, D., Failli, P., Bello, M. G., Thiemermann, C., Bani Sacchi, T., Bigazzi, M., and Masini, E. (1998) Relaxin activates the L-arginine-nitric oxide pathway in vascular smooth muscle cells in culture, *Hypertension 31*, 1240−1247.
38. Kim, Y. M., Chung, H. T., Simmons, R. L., and Billiar, T. R. (2000) Cellular non-heme iron content is a determinant of nitric oxide-mediated apoptosis, necrosis, and caspase inhibition, *J. Biol. Chem. 275*, 10954−10961.
39. Boese, M., Mordvintcev, P. I., Vanin, A. F., Busse, R., and Mulsch, A. (1995) S-Nitrosation of serum albumin by dinitrosyl-iron complex, *J. Biol. Chem. 270*, 29244−29249.
40. Kluge, I., Gutteck-Amsler, U., Zollinger, M., and Do, K. Q. (1997) S-Nitrosoglutathione in rat cerebellum: Identification and quantification by liquid chromatography-mass spectrometry, *J. Neurochem. 69*, 2599−2607.
41. Steffen, M., Sarkela, T. M., Gybina, A. A., Steele, T. W., Trasseth, N. J., Kuehl, D., and Giulivi, C. (2001) Metabolism of S-nitrosoglutathione in intact mitochondria, *Biochem. J. 356*, 395−402.
42. Jones, D. P. (2006) Extracellular redox state: Refining the definition of oxidative stress in aging, *Rejuvenation Res. 9*, 169−181.
43. Moslen, M. T., Kanz, M. F., Bhatia, J., Smith, C. V., and Rassin, D. K. (1994) Biliary glutathione and some amino acids are markedly diminished when biliary pressure is elevated, *Exp. Mol. Pathol. 61*, 1−15.
44. Inoue, K., Akaike, T., Miyamoto, Y., Okamoto, T., Sawa, T., Otagiri, M., Suzuki, S., Yoshimura, T., and Maeda, H. (1999) Nitrosothiol formation catalyzed by ceruloplasmin. Implication for cytoprotective mechanism in vivo, *J. Biol. Chem. 274*, 27069−27075.
45. Zhang, Y., and Hogg, N. (2004) The mechanism of transmembrane S-nitrosothiol transport, *Proc. Natl. Acad. Sci. U.S.A. 101*, 7891−7896.
46. Zhang, Y., and Hogg, N. (2005) S-Nitrosothiols: Cellular formation and transport, *Free Radical Biol. Med. 38*, 831−838.
47. Broniowska, K. A., Zhang, Y., and Hogg, N. (2006) Requirement of transmembrane transport for S-nitrosocysteine-dependent modification of intracellular thiols, *J. Biol. Chem. 281*, 33835−33841.
48. Li, S., and Whorton, A. R. (2005) Identification of stereoselective transporters for S-nitroso-L-cysteine: Role of LAT1 and LAT2 in biological activity of S-nitrosothiols, *J. Biol. Chem. 280*, 20102−20110.
49. Powis, G., and Montfort, W. R. (2001) Properties and biological activities of thioredoxins, *Annu. Rev. Biophys. Biomol. Struct. 30*, 421−455.
50. Yui, Y., Hattori, R., Kosuga, K., Eizawa, H., Hiki, K., and Kawai, C. (1991) Purification of nitric oxide synthase from rat macrophages, *J. Biol. Chem. 266*, 12544−12547.
51. Davisson, R. L., Travis, M. D., Bates, J. N., Johnson, A. K., and Lewis, S. J. (1997) Stereoselective actions of S-nitrosocysteine in central nervous system of conscious rats, *Am. J. Physiol. 272*, H2361−H2368.
52. Davisson, R. L., Travis, M. D., Bates, J. N., and Lewis, S. J. (1996) Hemodynamic effects of L- and D-S-nitrosocysteine in the rat. Stereoselective S-nitrosothiol recognition sites, *Circ. Res. 79*, 256−262.
53. Lipton, A. J., Johnson, M. A., Macdonald, T., Lieberman, M. W., Gozal, D., and Gaston, B. (2001) S-Nitrosothiols signal the ventilatory response to hypoxia, *Nature 413*, 171−174.
54. Lipton, S. A. (2001) Physiology. Nitric oxide and respiration, *Nature 413*, 118−119, 121.
55. Watson, W. H., Pohl, J., Montfort, W. R., Stuchlik, O., Reed, M. S., Powis, G., and Jones, D. P. (2003) Redox potential of human thioredoxin 1 and identification of a second dithiol/disulfide motif, *J. Biol. Chem. 278*, 33408−33415.

56. Haendeler, J., Hoffmann, J., Tischler, V., Berk, B. C., Zeiher, A. M., and Dimmeler, S. (2002) Redox regulatory and anti-apoptotic functions of thioredoxin depend on S-nitrosylation at cysteine 69, *Nat. Cell Biol. 4*, 743−749.
57. Mitchell, D. A., and Marletta, M. A. (2005) Thioredoxin catalyzes the S-nitrosation of the caspase-3 active site cysteine, *Nat. Chem. Biol. 1*, 154−158.
58. Weichsel, A., Brailey, J. L., and Montfort, W. R. (2007) Buried S-nitrosocysteine revealed in crystal structures of human thioredoxin, *Biochemistry 46*, 1219−1227.
59. Kabakibi, A., Morse, C. R., and Laposata, M. (1998) Fatty acid ethyl esters and HepG2 cells: Intracellular synthesis and release from the cells, *J. Lipid Res. 39*, 1568−1582.
60. Wolfla, C. E., Ross, R. A., and Crabb, D. W. (1988) Induction of alcohol dehydrogenase activity and mRNA in hepatoma cells by dexamethasone, *Arch. Biochem. Biophys. 263*, 69−76.
61. Jimenez-Lopez, J. M., Carrasco, M. P., Segovia, J. L., and Marco, C. (2002) Resistance of HepG2 cells against the adverse effects of ethanol related to neutral lipid and phospholipid metabolism, *Biochem. Pharmacol. 63*, 1485−1490.
62. Tyurina, Y. Y., Basova, L. V., Konduru, N. V., Tyurin, V. A., Potapovich, A. I., Cai, P., Bayir, H., Stoyanovsky, D., Pitt, B. R., Shvedova, A. A., Fadeel, B., and Kagan, V. E. (2007) Nitrosative stress inhibits the aminophospholipid translocase resulting in phosphatidylserine externalization and macrophage engulfment: Implications for the resolution of inflammation, *J. Biol. Chem. 282*, 8498−8509.
63. St Croix, C. M., Stitt, M. S., Watkins, S. C., and Pitt, B. R. (2005) Fluorescence resonance energy transfer-based assays for the real-time detection of nitric oxide signaling, *Methods Enzymol. 396*, 317−326.
64. Kim, Y. M., Talanian, R. V., and Billiar, T. R. (1997) Nitric oxide inhibits apoptosis by preventing increases in caspase-3-like activity via two distinct mechanisms, *J. Biol. Chem. 272*, 31138−31148.
65. Li, J., Billiar, T. R., Talanian, R. V., and Kim, Y. M. (1997) Nitric oxide reversibly inhibits seven members of the caspase family via S-nitrosylation, *Biochem. Biophys. Res. Commun. 240*, 419−424.
66. Bachrach, S. M., Woody, J. T., and Mulhearn, D. C. (2002) Effect of ring strain on the thiolate-disulfide exchange. A computational study, *J. Org. Chem. 67*, 8983−8990.
67. Tsikas, D., Sandmann, J., Rossa, S., Gutzki, F. M., and Frolich, J. C. (1999) Investigations of S-transnitrosylation reactions between low- and high-molecular-weight S-nitroso compounds and their thiols by high-performance liquid chromatography and gas chromatography-mass spectrometry, *Anal. Biochem. 270*, 231−241.
68. Hogg, N. (1999) The kinetics of S-transnitrosation: A reversible second-order reaction, *Anal. Biochem. 272*, 257−262.
69. Szajewski, R. P., and Whitesides, G. M. (1980) Rate constants and equilibrium constants for thiol-disulfide interchange reactions involving oxidized glutathione, *J. Am. Chem. Soc. 102*, 2011−2026.
70. Singh, R., and Whitesides, G. M. (1990) Degenerate intermolecular thiolate-disulfide interchange involving cyclic five-membered disulfides is faster by ∼103 than that involving six- or seven-membered disulfides, *J. Am. Chem. Soc. 112*, 6304−6309.
71. Chivers, P. T., Prehoda, K. E., Volkman, B. F., Kim, B. M., Markley, J. L., and Raines, R. T. (1997) Microscopic pKa values of *Escherichia coli* thioredoxin, *Biochemistry 36*, 14985−14991.
72. Vohnik, S., Hanson, C., Tuma, R., Fuchs, J. A., Woodward, C., and Thomas, G. J., Jr. (1998) Conformation, stability, and active-site cysteine titrations of *Escherichia coli* D26A thioredoxin probed by Raman spectroscopy, *Protein Sci. 7*, 193−200.
73. Stamler, J. S., Toone, E. J., Lipton, S. A., and Sucher, N. J. (1997) (S)NO signals: Translocation, regulation, and a consensus motif, *Neuron 18*, 691−696.
74. Ascenzi, P., Colasanti, M., Persichini, T., Muolo, M., Polticelli, F., Venturini, G., Bordo, D., and Bolognesi, M. (2000) Re-evaluation of amino acid sequence and structural consensus rules for cysteine-nitric oxide reactivity, *Biol. Chem. 381*, 623−627.
75. Chan, N. L., Rogers, P. H., and Arnone, A. (1998) Crystal structure of the S-nitroso form of liganded human hemoglobin, *Biochemistry 37*, 16459−16464.
76. Weichsel, A., Maes, E. M., Andersen, J. F., Valenzuela, J. G., Shokhireva, T., Walker, F. A., and Montfort, W. R. (2005) Heme-assisted S-nitrosation of a proximal thiolate in a nitric oxide transport protein, *Proc. Natl. Acad. Sci. U.S.A. 102*, 594−599.
77. Lopez-Sanchez, L. M., Collado, J. A., Corrales, F. J., Lopez-Cillero, P., Montero, J. L., Fraga, E., Serrano, J., De La Mata, M., Muntane, J., and Rodriguez-Ariza, A. (2007) S-Nitrosation of proteins during D-galactosamine-induced cell death in human hepatocytes, *Free Radical Res. 41*, 50−61.
78. Ji, Y., Akerboom, T. P., Sies, H., and Thomas, J. A. (1999) S-Nitrosylation and S-glutathiolation of protein sulfhydryls by S-nitroso glutathione, *Arch. Biochem. Biophys. 362*, 67−78.
79. Ckless, K., Reynaert, N. L., Taatjes, D. J., Lounsbury, K. M., van der Vliet, A., and Janssen-Heininger, Y. (2004) In situ detection and visualization of S-nitrosylated proteins following chemical derivatization: Identification of Ran GTPase as a target for S-nitrosylation, *Nitric Oxide 11*, 216−227.
80. Forsythe, P., and Befus, A. D. (2003) Inhibition of calpain is a component of nitric oxide-induced down-regulation of human mast cell adhesion, *J. Immunol. 170*, 287−293.
81. Chai, Y. C., Jung, C. H., Lii, C. K., Ashraf, S. S., Hendrich, S., Wolf, B., Sies, H., and Thomas, J. A. (1991) Identification of an abundant S-thiolated rat liver protein as carbonic anhydrase III: Characterization of S-thiolation and dethiolation reactions, *Arch. Biochem. Biophys. 284*, 270−278.
82. Tyagi, N., Moshal, K. S., Ovechkin, A. V., Rodriguez, W., Steed, M., Henderson, B., Roberts, A. M., Joshua, I. G., and Tyagi, S. C. (2005) Mitochondrial mechanism of oxidative stress and systemic hypertension in hyperhomocysteinemia, *J. Cell. Biochem. 96*, 665−671.
83. Lemaire, S. D., Guillon, B., Le Marechal, P., Keryer, E., Miginiac-Maslow, M., and Decottignies, P. (2004) New thioredoxin targets in the unicellular photosynthetic eukaryote *Chlamydomonas reinhardtii*, *Proc. Natl. Acad. Sci. U.S.A. 101*, 7475−7480.
84. Zuckerbraun, B. S., Stoyanovsky, D. A., Sengupta, R., Shapiro, R. A., Ozanich, B. A., Rao, J., Barbato, J. E., and Tzeng, E. (2007) Nitric oxide-induced inhibition of smooth muscle cell proliferation involves S-nitrosation and inactivation of RhoA, *Am. J. Physiol. 292*, C824−C831.
85. Zech, B., Wilm, M., van Eldik, R., and Brune, B. (1999) Mass spectrometric analysis of nitric oxide-modified caspase-3, *J. Biol. Chem. 274*, 20931−20936.
86. Svingen, P. A., Loegering, D., Rodriquez, J., Meng, X. W., Mesner, P. W., Jr., Holbeck, S., Monks, A., Krajewski, S., Scudiero, D. A., Sausville, E. A., Reed, J. C., Lazebnik, Y. A., and Kaufmann, S. H. (2004) Components of the cell death machine and drug sensitivity of the National Cancer Institute Cell Line Panel, *Clin. Cancer Res. 10*, 6807−6820.
87. Corradi, M., Montuschi, P., Donnelly, L. E., Pesci, A., Kharitonov, S. A., and Barnes, P. J. (2001) Increased nitrosothiols in exhaled breath condensate in inflammatory airway diseases, *Am. J. Respir. Crit. Care Med. 163*, 854−858.
88. Nakamura, T., and Lipton, S. A. (2007) S-Nitrosylation and uncompetitive/fast off-rate (UFO) drug therapy in neurodegenerative disorders of protein misfolding, *Cell Death Differ.* (in press).
89. Grattagliano, I., Portincasa, P., Palmieri, V. O., and Palasciano, G. (2007) Mutual changes of thioredoxin and nitrosothiols during biliary cirrhosis: Results from humans and cholestatic rats, *Hepatology 45*, 331−339.
90. Doyle, M. P., Mahapatro, S. N., Broene, R. D., and Guy, J. K. (1988) Oxidation and reduction of hemoproteins by trioxodinitrate-(II). The role of nitrosyl hydride and nitrite, *J. Am. Chem. Soc. 110*, 593−599.
91. Liochev, S. I., and Fridovich, I. (2003) The mode of decomposition of Angeli's salt ($Na_2N_2O_3$) and the effects thereon of oxygen, nitrite, superoxide dismutase, and glutathione, *Free Radical Biol. Med. 34*, 1399−1404.
92. Miranda, K. M., Paolocci, N., Katori, T., Thomas, D. D., Ford, E., Bartberger, M. D., Espey, M. G., Kass, D. A., Feelisch, M., Fukuto, J. M., and Wink, D. A. (2003) A biochemical rationale for the discrete behavior of nitroxyl and nitric oxide in the cardiovascular system, *Proc. Natl. Acad. Sci. U.S.A. 100*, 9196−9201.
93. Nelli, S., McIntosh, L., and Martin, W. (2001) Role of copper ions and cytochrome P450 in the vasodilator actions of the nitroxyl anion generator, Angeli's salt, on rat aorta, *Eur. J. Pharmacol. 412*, 281−289.

94. Nelli, S., Hillen, M., Buyukafsar, K., and Martin, W. (2000) Oxidation of nitroxyl anion to nitric oxide by copper ions, *Br. J. Pharmacol. 131*, 356−362.
95. Nagasawa, H. T., DeMaster, E. G., Redfern, B., Shirota, F. N., and Goon, D. J. (1990) Evidence for nitroxyl in the catalase-mediated bioactivation of the alcohol deterrent agent cyanamide, *J. Med. Chem. 33*, 3120−3122.
96. Favaloro, J. L., and Kemp-Harper, B. K. (2007) The nitroxyl anion (HNO) is a potent dilator of rat coronary vasculature, *Cardiovasc. Res. 73*, 587−596.
97. Ma, X. L., Gao, F., Liu, G. L., Lopez, B. L., Christopher, T. A., Fukuto, J. M., Wink, D. A., and Feelisch, M. (1999) Opposite effects of nitric oxide and nitroxyl on postischemic myocardial injury, *Proc. Natl. Acad. Sci. U.S.A. 96*, 14617−14622.
98. Paolocci, N., Katori, T., Champion, H. C., St John, M. E., Miranda, K. M., Fukuto, J. M., Wink, D. A., and Kass, D. A. (2003) Positive inotropic and lusitropic effects of HNO/NO^- in failing hearts: Independence from β-adrenergic signaling, *Proc. Natl. Acad. Sci. U.S.A. 100*, 5537−5542.
99. Ivanova, J., Salama, G., Clancy, R. M., Schor, N. F., Nylander, K. D., and Stoyanovsky, D. A. (2003) Formation of nitroxyl and hydroxyl radical in solutions of sodium trioxodinitrate: Effects of pH and cytotoxicity, *J. Biol. Chem. 278*, 42761−42768.
100. Stoyanovsky, D. A., Schor, N. F., Nylander, K. D., and Salama, G. (2004) Effects of pH on the cytotoxicity of sodium trioxodinitrate (Angeli's salt), *J. Med. Chem. 47*, 210−217.
101. Kim, W. K., Choi, Y. B., Rayudu, P. V., Das, P., Asaad, W., Arnelle, D. R., Stamler, J. S., and Lipton, S. A. (1999) Attenuation of NMDA receptor activity and neurotoxicity by nitroxyl anion, NO, *Neuron 24*, 461−469.

BI700449X